Journal of Membrane Science 525 (2017) 18–24

Contents lists available at ScienceDirect

Journal of Membrane Science

journal homepage: www.elsevier.com/locate/memsci

Analysis of the transport properties of thermally rearranged (TR) polymers and polymers of intrinsic microporosity (PIM) relative to upper bound performance

Lloyd M. Robeson[a], Michelle E. Dose[b,*], Benny D. Freeman[b], Donald R. Paul[b]

[a] Department of Materials Science and Engineering, Lehigh University, 1801 Mill Creek Road, Macungie, PA 18062, USA
[b] Department of Chemical Engineering, Texas Materials Institute, Center for Energy and Environmental Research, Center for Research in Water Resources, The University of Texas at Austin, 10100 Burnet Road, Bldg 133, Austin, TX 78758, USA

ARTICLE INFO

Keywords:
Thermally rearranged
Polymers of intrinsic microporosity
Polymer upper bound
Diffusion
Solubility
Permeability
O_2/N_2
CO_2/CH_4

ABSTRACT

A critical analysis comparing the diffusion selectivity, solubility selectivity, diffusivity, and solubility coefficients of thermally rearranged (TR) polymers and polymers of intrinsic microporosity (PIM), two types of polymers which consistently perform at or beyond the polymer upper bound for certain gas pairs (O_2/N_2 and CO_2/CH_4), is reported here. Although most polymers in these two classes exhibit transport properties in the range of typical glassy polymers, several variants offer exceptional performance. The diffusivity selectivity for O_2/N_2 and CO_2/CH_4 for TR polymers and PIM lies outside the range of the glassy polymer database. The solubility coefficients for O_2 are at the upper end of the range of both TR and PIM polymers, as is also the case for CO_2 solubility coefficients for PIM polymers. The O_2/N_2 and CO_2/CH_4 solubility selectivities for both PIM and TR polymers are in the range of typical glassy polymers. Thus, unique separation values for these polymers are a manifestation of maximizing diffusivity selectivity combined with very high gas solubility. Additionally, the previously determined diffusion gas kinetic diameters, d_g, were found to correlate best with diffusion coefficients of PIM and TR polymers and serve to better analyze transport properties of upper bound materials.

1. Introduction

Polymer membranes were first used for gas phase separations on a commercial scale in the late 1970s by Permea, now Air Products and Chemicals Inc., with the use of their Prism® membranes systems for hydrogen recovery from ammonia plant purge streams [1–3]. As of 2016, commercial membrane systems are now employed in many applications, including separation of gas pairs such as O_2/N_2, CO_2/CH_4, H_2/N_2, H_2/CO_2, He/air, and H_2O/natural gas [1–5].

The limits of polymer membrane performance for gas separations has been defined by a relationship termed the "upper bound" [6,7]. The upper bound is an empirical relationship from a log-log plot of ideal permselectivity (α_{ij}) versus permeability (P_i), where i represents the more permeable component of the gas pair i and j, and α_{ij} is defined as the ratio of gas pair permeability values (P_i/P_j). On these plots, an upper bound line can be drawn above which virtually no data exist, indicating there is a trade-off between permeability and selectivity. In 1999, this empirical relationship was supported by a theoretical prediction of the upper bound parameters by Freeman [6,8]. To delve further into the fundamental properties that lead to this trade-off, the permeability, diffusivity (D), and solubility (S) values for a large database of glassy polymers were evaluated. The diffusivity selectivity (D_i/D_j) was determined to be the primary factor in establishing the slope of the upper bound, while the solubility selectivity (S_i/S_j) had only a modest contribution [9]. Additionally, the gas pair solubility selectivity decreases with increasing free volume and permeability when the diameter of the more permeable gas, i, is smaller than that of the less permeable gas, j[9]. Analysis of the diffusion data in glassy polymers yielded a set of gas diameters that were hypothesized to be more relevant for correlating gas diffusion in polymers than prior determinations. In a more recent paper, it was shown that while diffusion coefficients determine the slope of the upper bound, glassy polymers, as opposed to rubbery polymers, tend to dominate the upper bound due to higher solubility coefficient values [10].

Two classes of polymers, in particular, exhibit upper bound properties for many gas pairs and exceed upper bound performance in some cases (e.g., O_2/N_2 and CO_2/CH_4). These groups of polymers are generally referred to as polymers of intrinsic microporosity (PIM) [11–34] and thermally rearranged (TR) polymers [35–44].

PIM were initially investigated by Budd, McKeown and coinvesti-

* Corresponding author.
E-mail address: m.dose@utexas.edu (M.E. Dose).

http://dx.doi.org/10.1016/j.memsci.2016.11.085
Received 20 September 2016; Received in revised form 29 November 2016; Accepted 30 November 2016
Available online 02 December 2016

gators at the University of Manchester [11–17,21]. Their synthesis of "ladder" type polymers of intrinsic microporosity (defined as containing interchain spacing or "pores" of < 2 nm) revealed gas separation properties with high gas permeability and upper bound selectivity. The rigid polybenzodioxane backbones of these polymers result in poor molecular packing and thus exhibit high free volume. The upper bound performance of these polymers was attributed to high gas solubility, allowing increased permeability without sacrificing selectivity [15]. This view agrees with the observation that glassy polymers dominate the upper bound, relative to rubbery polymers, due to the dual mode sorption behavior of glassy polymers [10].

Thermally rearranged (TR) polybenzoxazole polymers, initially reported by Lee and coinvestigators, have also generated significant interest for gas separation membranes, specifically for CO_2 based separations [35]. Due to the low solubility of polybenzoxazoles, TR polymers are traditionally formed by the solid state thermal conversion of hydroxyl-containing polyimides to polybenzoxazoles at temperatures ranging from 300 to 450 °C for a prescribed time [45,46]. The exceptional CO_2/CH_4 selectivity and high permeability of the initial materials were attributed to "well-tuned" cavity formation during thermal rearrangement process. Positron annihilation lifetime spectroscopy (PALS) lent credence to this concept by showing a narrow distribution of the free volume or pore structure after rearrangement.

A critical analysis of the diffusion selectivity, solubility selectivity, diffusion coefficients, and solubility coefficients of PIM and TR polymers, as compared with other glassy polymers, is detailed in this paper. A large database of permeability, diffusivity, and solubility data for glassy polymers for the analysis in a previous study was employed in this work [9]. While TR polymers and PIM materials perform at or beyond the upper bound for several different gas pairs, O_2/N_2 and CO_2/CH_4 were used for this analysis due to the widespread availability of permeability, solubility, and diffusivity data for O_2, N_2, CO_2 and CH_4, and the lack of necessary data for other gases.

2. Analysis of the transport properties of PIM and TR polymers

Permeability data reported for PIM [15,20,22–34] and TR polymers [36,43,44,47–50] are compared for O_2/N_2 and CO_2/CH_4 separations in Figs. 1 and 2, respectively. For each case, the data are compared with the appropriate empirical 2008 upper bound [7]. Both PIM and TR polymers have data points above the upper bound

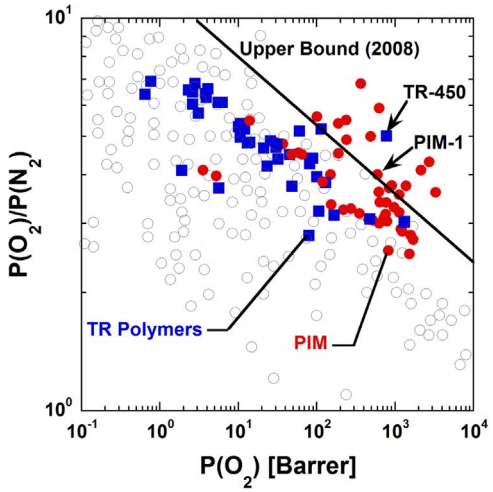

Fig. 1. Upper bound relationship for PIM (red circles) and TR polymers (blue squares) for O_2/N_2 separation. The unfilled circles represent glassy polymers from a previously reported database [9]. The data points for TR-450 [43] and PIM-1 [16] have been highlighted with arrows. (For interpretation of the references to color in this figure legend, the reader is referred to the web version of this article.)

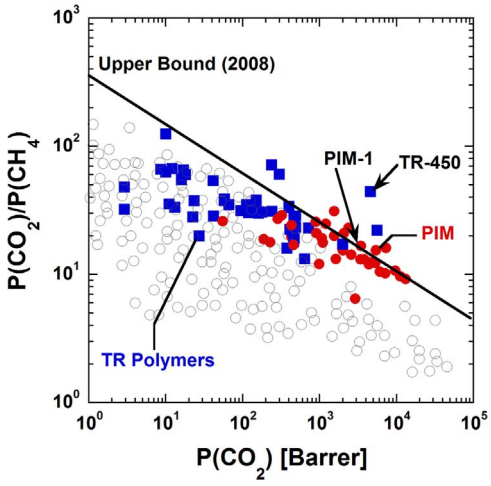

Fig. 2. Upper bound relationship for PIM (red circles) and TR polymers (blue squares) for CO_2/CH_4 separation. The unfilled circles represent glassy polymers from a previously reported database [9]. The data points for TR-450 [43] and PIM-1 [16] have been highlighted with arrows. (For interpretation of the references to color in this figure legend, the reader is referred to the web version of this article.)

for O_2/N_2 while predominately TR polymers exceed the upper bound for CO_2/CH_4. However, most of the data reported for PIM and TR polymers are close to but below the upper bound relationship, with the exception of a few recently developed PIM materials which significantly exceed the upper bound [27,29,30,32–34]. Some of the PIM variants reported were used to establish the empirical 2008 upper bound [7] and recently, due to the excellent performance of newly developed PIM materials, Swaidan et al. have proposed a new 2015 upper bound for O_2/N_2 separation [28]. While several TR polymers exceed the 2008 upper bound, TR polymers are not solution-processable and therefore are not formally used to determine the position of the Robeson upper bounds. To serve as reference points, PIM-1 [16] and TR-450 [43] polymers have been highlighted in many of the following figures. PIM-1 is a heavily studied polymer of intrinsic microporosity formed from the condensation of 5,5′,6,6′-tetrahydroxy-3,3,3′,3′-tetramethyl-1,1′-spirobisindane and tetrafluoroterephthalonitrile. The data used in the remainder of this work is for PIM-1 treated with methanol [16]. TR-450 is the polymer formed from the thermal treatment of a hydroxyl-containing polyimide based off of 2,2-bis(3-amino-4-hydroxyphenyl)-hexafluoropropane (bisAPAF) and 4,4′-hexafluoroisopropylidene diphthalic anhydride (6FDA) moieties, heated at 450 °C for 1 h.

In a previous paper [10], gas diffusion coefficients (D) for rubbery and glassy polymers were compared by correlating data sets using the following equation:

$$lnD=\alpha+\beta d_g^2 \quad (1)$$

where α and β are fit for each polymer data set, and β serves as a measure of the size sieving ability of the polymer. The gas diameters, d_g, were determined in reference [9] by analysis of diffusion in glassy polymers, which provided a prediction of the gas diameters of He, H_2, O_2, N_2, and CO_2 once the diameter of CH_4 was fixed. By plotting the diffusion coefficients for a gas of intermediate diameter (O_2, d_g =3.23 Å) as a function of the slope, β, as defined by Eq. (1), considerable overlap in the data for glassy and rubbery polymers suggested only modest differences in the diffusion selectivity between the two different polymer classes [10]. This deeper analysis of diffusion coefficients contradicted previous beliefs that glassy polymers dominated the upper bound due to higher diffusivity selectivity than rubbery polymers [9,10]. This analysis has been extended to this study, as shown in Fig. 3. Additional data have been added to the previous analysis [10], where diffusion values of at least 5 of the 6 mentioned gases have been reported [51–61]. Values for PIM [15,22–33], TR

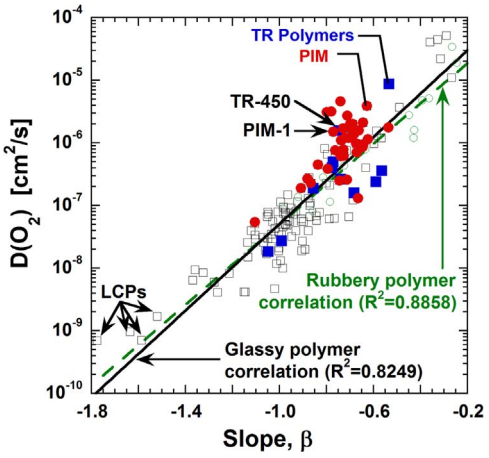

Fig. 3. Correlation of glassy (black unfilled squares) and rubbery (green unfilled circles) polymer data for oxygen diffusion coefficients (d_g =3.25 Å) from Eq. (1)[10], with PIM (red circles) and TR polymers (blue squares) highlighted to indicate agreement with previous analysis. Liquid crystalline polymers (LCPs), TR-450, and PIM-1 are indicated by arrows. (For interpretation of the references to color in this figure legend, the reader is referred to the web version of this article.)

polymers [36,43,44], and liquid crystalline polymers (LCPs) [51,61,62] have also been included to provide a comparison for gas diffusivity in polymers with high and very low permeabilities. Each point on the plot represents a polymer from the indicated data set. As in the previous paper, the glassy and rubbery polymer correlation lines are quite similar [10]. Thus, the diffusion selectivity of glassy and rubbery polymers are not as different as once believed, even for upper bound materials such as PIM and TR polymers. The data points for TR-450 and PIM-1, highlighted in Fig. 3, lie above the glassy polymer correlation. Thus, both families of materials have diffusion coefficients significantly higher than other polymers of similar β value (i.e., similar size sieving ability). For this reason, PIM-1 [16] and TR-450 [43] have been selected to represent the PIM and TR polymer data sets. Liquid crystalline polymers also exhibit higher diffusion coefficients versus the correlation line at the lower end of the permeability range.

Fig. 4 presents a comparison of diffusion coefficients for TR-450 and PIM-1 versus gas diameter. The gas diameter values utilized for this figure were those noted for Fig. 3 and reported in reference [10]. As predicted by Eq. (1), the diffusion coefficients follow a linear correlation with gas diameter squared, and there is no discernible

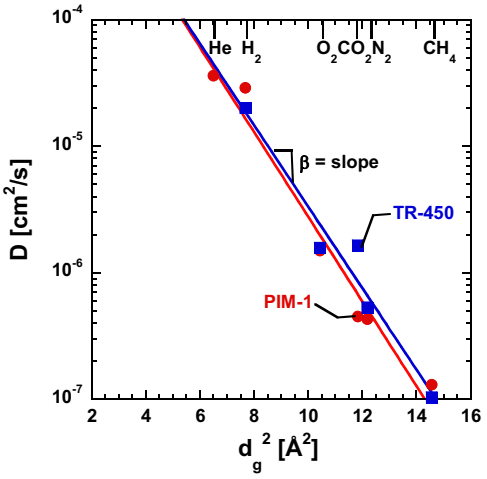

Fig. 4. Diffusion coefficients versus gas diameter squared (d_g^2) for PIM-1 (red circles) and TR-450 (blue squares). The specific expressions of Eq. (1) for TR-450 [43]. The parameters for the shown linear fits to Eq. (1) are included in Table 1. (For interpretation of the references to color in this figure legend, the reader is referred to the web version of this article.)

Table 1
Parameters for Eq. (1) used to correlate diffusion coefficients (cm^2/s) for PIM-1 and TR-450 versus the gas diffusion diameters, d_g (Å^2). The parameters and uncertainties were determined assuming a 10% uncertainty in the diffusion coefficient values and a least square fit analysis.

Material	α	β	R^2
PIM-1	−5.3 ± 0.2	−0.75 ± 0.01	0.968
TR-450	−5.2 ± 0.2	−0.74 ± 0.02	0.955

difference between the trends for PIM-1 and TR-450. The parameters fitting Eq. (1) to PIM-1 and TR-450 diffusion coefficients are included in Table 1. These results agree with previous observations [9] that the dependence of gas diffusion coefficients on the square of gas diameters (i.e., β in Eq. (1)) is similar when polymers have similar diffusion coefficients. Interestingly, the diffusion coefficient of CO_2 (d_g^2 =11.8 Å^2) in TR-450 lies significantly above the linear correlation. This deviation may contribute to the fact that TR-450 exceeds the 2008 upper bound properties for CO_2/CH_4 separation (cf., Fig. 2) [7].

PIM and TR polymers are often reported to have transport properties near or above the upper bound for the O_2/N_2 and CO_2/CH_4 gas pairs. The diffusivity selectivity for PIM and TR polymers are compared to the rest of the glassy polymer database in Figs. 5 and 6 for O_2/N_2 and CO_2/CH_4, respectively. As expected, the glassy polymer data show a distinct upper bound relationship for both gas pairs in log-log plots of diffusivity selectivity (D_i/D_j) versus diffusivity of the faster component (D_i). Similar to the permeability upper bound (cf., Fig. 1), several PIM and TR polymers lie on or above the diffusivity upper bound for O_2/N_2. For CO_2/CH_4 separation, several TR polymers show equal or higher diffusivity selectivity than the glassy polymer diffusivity upper bound, while PIM have properties comparable to those of other glassy polymers. Power law fits for D_i/D_j with respect to D_i (i.e., $\log\left(\frac{D_i}{D_j}\right)=A\log(D_i)+B$) have been included for all data points in Figs. 5 and 6 to show the general trend of decreasing diffusion selectivity with increasing diffusivity.

The solubility data for PIM [11–34] and TR polymers [35–44] were obtained from the references noted earlier. A plot of solubility constants versus permeability coefficients is shown for O_2 solubility (Fig. 7) and CO_2 solubility (Fig. 8). These data are compared with similar data for other glassy polymers from reference [9]. All data shown fall within the trend noted previously [9], where the solubility coefficients generally increase with increasing permeability. However,

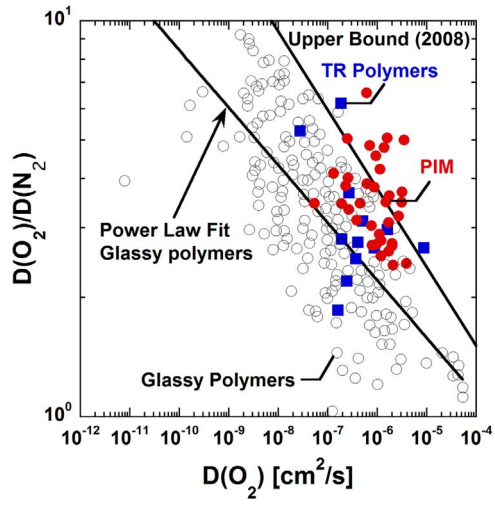

Fig. 5. Diffusivity upper bound correlation for O_2/N_2, comparing PIM (red circles) and TR polymers (blue squares) to the glassy polymer database (unfilled circles) [9]. (For interpretation of the references to color in this figure legend, the reader is referred to the web version of this article.)

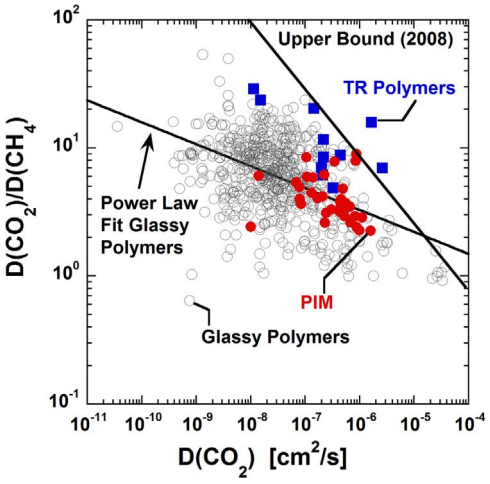

Fig. 6. Diffusivity upper bound correlation for CO_2/CH_4, comparing PIM (red circles) and TR polymers (blue squares) to the glassy polymer database (unfilled circles) [9]. (For interpretation of the references to color in this figure legend, the reader is referred to the web version of this article.)

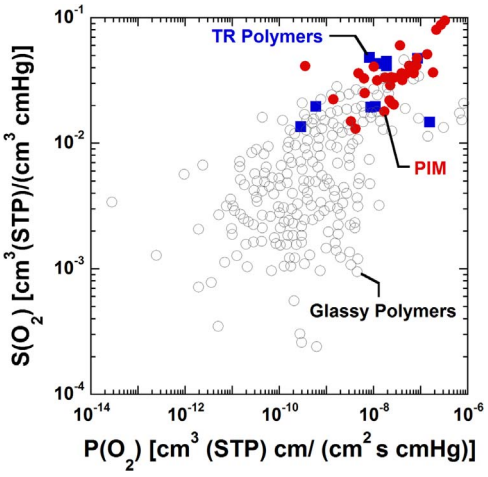

Fig. 7. Comparison of O_2 solubility coefficient data of PIM (red circles) and TR variants (blue squares) with the glassy polymer database (unfilled circles) [9]. (For interpretation of the references to color in this figure legend, the reader is referred to the web version of this article.)

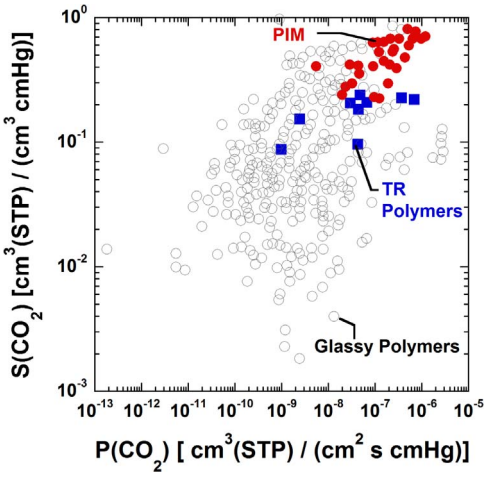

Fig. 8. Comparison of CO_2 solubility coefficient data of PIM (red circles) and TR polymers (blue squares) with the glassy polymer database (unfilled circles) [9]. (For interpretation of the references to color in this figure legend, the reader is referred to the web version of this article.)

Table 2
O_2/N_2 and CO_2/CH_4 gas pair selectivity values for glassy polymers, PIM, and TR polymers. The indicated references denote which data sets were used to obtain the average value and range shown.

	S (O_2)/S (N_2)		S (CO_2)/S (CH_4)	
Polymer	**Average**	**Range**	**Average**	**Range**
glassy polymers[9]	1.30	0.31–2.50	5.00	0.93–47.5
PIM[15,22–24]	1.16	1.03–1.44	4.35	3.19–5.09
TR polymers[36,43,44]	1.39	1.05–1.83	3.02	2.50–4.30

both PIM and TR polymers show O_2 solubility values towards the higher end of the trend. Additionally, PIM materials exhibit higher CO_2 solubility coefficients relative to the spread of the data for glassy polymers, while TR polymers have values scattered within the glassy polymer data set. Compared to other glassy polymers, TR polymers and PIM have both high solubility and diffusivity coefficients. These "upper limit" transport properties contribute significantly to the upper bound behavior of these two polymer classes.

The gas pair selectivities (S_i/S_j) were calculated for PIM and TR polymers. The results are summarized in Table 2, where the average and range of solubility selectivity values are reported. These results indicate both PIM and TR polymers have solubility selectivities within the general range of glassy polymers. This supports the previous analysis that high solubility, rather than solubility selectivity, contributes to polymers dominating upper bound behavior.

3. Correlation of PIM and TR polymer diffusion data with gas diameter

Correlations of gas diffusion coefficients in polymers with gas molecular dimensions (i.e., diameter squared or gas molecule volume) have been often reported in the literature. Grün, and several others since, have correlated diffusion coefficients with van der Waals molecular volume for a variety of gas permeants, ranging from He to n-hexane, in both polymers and solvents [63,64]. However, for small molecules, this correlation tends to be weak due to the non-sphericali nature of gas molecules like H_2, O_2, N_2, and CO_2. For this reason, several prominent correlations relating diffusion coefficients to the gas kinetic diameter exist. These include: the kinetic diameter determined from zeolite data (Breck diameters) [65], the Lennard-Jones gas diameter and collision diameter [66,67], the effective diameter [59], the Dal-Cin correlation diameter from analysis of the upper bound [68], the permeability correlation diameter [69], the Teplyakov-Meares (T-M) diameter [70], and the diffusion correlation diameter determined from glassy polymer data [9]. The Teplyakov-Meares (T-M) diameter correlation comprises a comprehensive list of gas diameters based on analysis of noble gas diffusion in a series of polymers to yield a fit to Eq. (1). While several of these correlations use the diameter of methane (a relatively spherical molecule) as a reference point, the T-M correlation used noble gases [70]. This choice resulted in diameters significantly lower than the other noted correlations (cf.,Table 3). While the absolute values of the T-M diameters are lower, the correlation ability to fit the gas diffusion data to the relative *difference in the diameter squared* is the key factor, not the magnitude of the gas diameter values. A comparison of the gas diameters utilized to correlate diffusion data is shown in Table 3.

The literature database for glassy [9] and rubbery polymers [10] yields the following relationship for diffusion coefficients: D(He) > $D(H_2)$ > $D(O_2)$ > $D(CO_2)$ > $D(N_2)$ > $D(CH_4)$. The closest proximity for the gas pairs is with $D(CO_2)$ and $D(N_2)$, with $D(CO_2)$ only slightly higher than $D(N_2)$. Four of the noted gas diameter correlations show this trend with the diameter of CO_2 being only slightly smaller than N_2. These include the T-M diameter, effective diameter, Dal-Cin correlation diameter, and the diffusion correlation diameter. While the perme-

Table 3
Gas diameters determined by different methods reported in the literature.

Gas	Gas Diameter (Å)							
	Teplyakov-Meares (T-M) [70]	Lennard-Jones[67]	Dal-Cin[68]	Lennard-Jones Collision[66]	Permeability[69]	Breck[65]	Effective[59]	Diffusion, d_g[9]
He	1.78	2.551	2.555	2.576	2.644	2.6	2.59	2.55
H_2	2.14	2.827	2.854	2.915	2.875	2.89	2.90	2.77
O_2	2.89	3.467	3.374	3.433	3.347	3.46	3.44	3.23
CO_2	3.02	3.941	3.427	3.996	3.325	3.3	3.63	3.44
N_2	3.04	3.798	3.588	3.681	3.568	3.64	3.66	3.49
CH_4	3.18	3.758	3.882	3.822	3.817	3.8	3.81	3.817

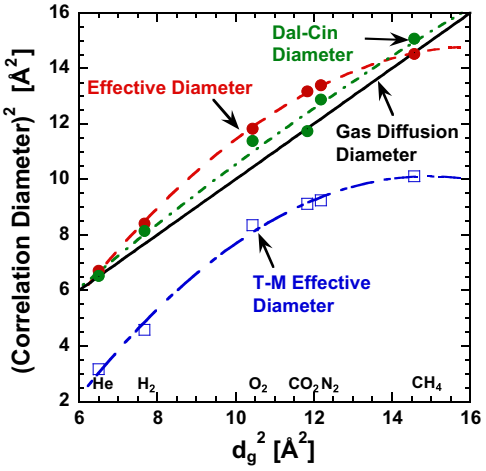

Fig. 9. Comparison of the effective [59], Dal-Cin [68], and Teplyakov-Meares [70] diameter correlations to the gas diffusion correlation diameter squared (d_g^2) [9]. A parity line (the solid, straight line) for the gas diffusion correlation diameter has been included as a reference.

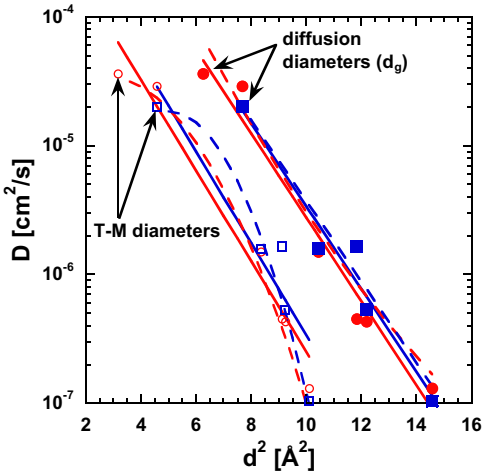

Fig. 10. Comparison of the fit of Eq. (1) for PIM-1 (red circles) [16] and TR-450 (blue squares) [43] employing the T-M diameters (unfilled markers) and the diffusion correlation diameters (filled markers). A linear fit (solid line) and a quadratic fit (dashed line) are shown for each correlation. The linear and quadratic fit parameters are listed in Table S1.

ability [69] and Breck [65] correlations give the diameters for CO_2 and N_2 in the appropriate size order, the differences are too large to reflect the small observed difference in diffusion coefficients. A comparison of these diameters (squared) plotted against the diffusion correlation diameter (d_g) is shown in Fig. 9 with a polynomial fit of the data. The comparison illustrated in Fig. 9 shows convex behavior for the effective diameter and the T-M diameter relative to the diffusion correlation diameter (all squared). The Dal-Cin diameter is quite close to linearity but shows a slight deviation for CO_2.

A comparison of the diffusion correlation diameter and the T-M diameter is presented in Fig. 10 with diffusion coefficient data for PIM-1 and TR-450. A linear fit of the data as well as a quadractic fit are shown, and a statistical assessment of these fits has been performed in the Supporting Information. Good linearity, as predicted by Eq. (1), is observed for the diffusion correlation diameter data, whereas convex behavior is observed for the T-M diameter data. The linear behavior is also observed with several other TR polymers as shown in Fig. 11. While the TR and PIM polymers better obey correlations with the diffusion correlation diameters, the T-M diameters often yield a better fit, as compared to d_g, with typical rubbery and non-upper bound glassy polymers. The gas diffusion correlation diameter (based only on glassy polymer data) often yields modestly concave behavior for ln(D) versus d_g^2 plots for rubbery and non-upper bound glassy polymers. The better fit of the TR and PIM diffusivities with the diffusion correlation diameters than with diameters from other correlations appears to be a consequence of the larger relative gas diameter difference between O_2, N_2, and CH_4 in d_g than in the other correlations.

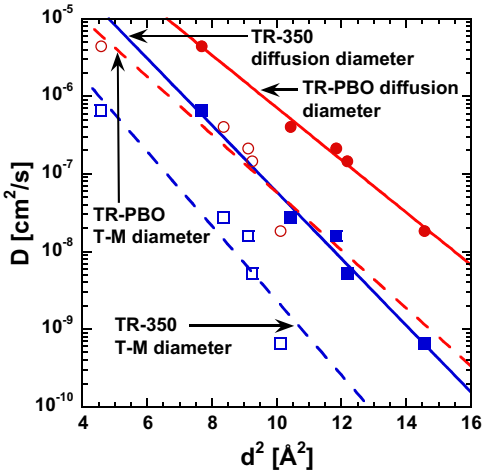

Fig. 11. Comparison of TR-PBO (red circles) and TR-350 (blue squares) diffusion data [43] fit with Eq. (1) employing the T-M diameters (open markers) and the diffusion correlation diameters (filled markers). Linear correlations for each data set are included. TR-350 is a TR polymer treated at 350 °C for 1 h for partial conversion to the PBO structure, and TR-PBO is a polymer treated at 450 °C for 1 h to achieve 100% conversion to the PBO structure [43].(For interpretation of the references to color in this figure legend, the reader is referred to the web version of this article.)

4. Conclusions

The transport properties of PIM and TR polymers variants have been compared with the spread of data for glassy polymers [71]. The diffusivity selectivity of common gases for specific TR and PIM variants

is modestly higher than most glassy polymers. For specific gas pairs (i.e., O_2/N_2 and CO_2/CH_4), some TR and PIM variants also offer higher diffusivity selectivity than other glassy polymers when compared on a diffusivity selectivity upper bound plot (i.e., $\log(D_i/D_j)$ versus D_i), although most of the variants are in the range of other glassy polymers. The natural log diffusion coefficient versus gas diameter squared correlations (i.e., Eq. (1)) is best fit by the diffusion correlation diameters, d_g, than by various other gas diameter correlations commonly employed for polymers.

The solubility coefficients of PIM variants for O_2 and CO_2 are in the higher range of the spread of glassy polymer data. TR variants show higher O_2 solubility coefficients relative to other glassy polymers but have CO_2 solubility coefficients more in the range of other glassy polymers. The O_2/N_2 and CO_2/CH_4 solubility selectivities for both PIM and TR variants are in the expected range for glassy polymers.

The basic conclusion from this analysis is that the upper bound performance (i.e., combination of high permeability and permeability selectivity) for specific PIM and TR polymers is due to a *combination* of higher diffusion selectivity, high diffusion coefficients, and high solubility coefficients, relative to other glassy polymers. The high solubility coefficients are a consequence of high free volume combined with high glass transition temperatures, leading to significant dual mode sorption, as noted previously [9]. Elevated solubility shifts the data to higher permeability values relative to other polymers at a given selectivity on the upper bound plots. This point has been recognized in an earlier hypothesis on PIM variants [15] and further supported by the evidence presented in this study. Thus, the excellent performance of TR and PIM variants is a consequence of maximizing diffusion selectivity, diffusion coefficients, and gas solubility. They appear to fit the solution-diffusion model and are not uniquely different in their transport mechanism than other polymers. Thus, upper bound behavior can be achieved when diffusion selectivity, diffusion coefficients, and gas solubility are simultaneously maximized.

Acknowledgements

This material is based upon work supported by the National Science Foundation Graduate Research Fellowship under Grant No. DGE-1610403. Additionally, the authors gratefully acknowledge support from the Division of Chemical Sciences, Geosciences, and Biosciences, Office of Basic Energy Sciences of the U.S. Department of Energy (DOE),USA through Grant DE-FG02-02ER15362.

Appendix A. Supporting information

Supplementary data associated with this article can be found in the online version at doi:10.1016/j.memsci.2016.11.085.

References

[1] J.M.S. Henis, Commercial and Practical Aspects of Gas Separation Membranes, in: D.R. Paul, Y.P. Yampol'skii (Eds.), Polymeric Gas Separation Membranes, CRC Press, Boca Raton, FL, 1994, pp. 442–468.
[2] R.W. Baker, Membrane Technology and Applications, in: Membrane Technology, John Wiley & Sons, Ltd, Chichester, UK, 2004, p. 545.
[3] W.A. Bollinger, D.L. MacLean, R.S. Narayan, Separation systems for oil refining and production, Chem. Eng. Prog. 78 (1982) 27–32.
[4] D.F.Sanders, Z.P.Smith, R.Guo, L.M.Robeson, J.E.McGrath, D.R.Paul, B.D. Freeman, Energy-efficient polymeric gas separation membranes for a sustainable future: A review, in:Polymer (United Kingdom)pp. 4729–4761, 2013.
[5] Y. Yampolskii, Polymeric gas separation membranes, Macromolecules 45 (2012) 3298–3311.
[6] L.M. Robeson, Correlation of separation factor versus permeability for polymeric membranes, J. Membr. Sci. 62 (1991) 165–185.
[7] L.M. Robeson, The upper bound revisited, J. Membr. Sci. 320 (2008) 390–400.
[8] B.D. Freeman, Basis of permeability/selectivity tradeoff relations in polymeric gas separation membranes, Macromolecules 32 (1999) 375–380.
[9] L.M. Robeson, Z.P. Smith, B.D. Freeman, D.R. Paul, Contributions of diffusion and solubility selectivity to the upper bound analysis for glassy gas separation membranes, J. Membr. Sci. 453 (2014) 71–83.
[10] L.M. Robeson, Q. Liu, B.D. Freeman, D.R. Paul, Comparison of transport properties of rubbery and glassy polymers and the relevance to the upper bound relationship, J. Membr. Sci. 476 (2015) 421–431.
[11] N.B. McKeown, S. Hanif, K. Msayib, C.E. Tattershall, P.M. Budd, Porphyrin-based nanoporous network polymers, Chem. Commun. (2002) 2782–2783.
[12] P.M. Budd, B. Ghanem, K. Msayib, N.B. McKeown, C. Tattershall, A nanoporous network polymer derived from hexaazatrinaphthylene with potential as an adsorbent and catalyst support, J. Mater. Chem. 13 (2003) 2721–2726.
[13] P.M. Budd, B.S. Ghanem, S. Makhseed, N.B. McKeown, K.J. Msayib, C.E. Tattershall, Polymers of intrinsic microporosity (PIMs): robust, solution-processable, organic nanoporous materials, Chem. Commun. (2004) 230–231.
[14] P.M. Budd, E.S. Elabas, B.S. Ghanem, S. Makhseed, N.B. McKeown, K.J. Msayib, C.E. Tattershall, D. Wang, Solution-processed, organophilic membrane derived from a polymer of intrinsic microporosity, Adv. Mater. 16 (2004) 456–459.
[15] P.M. Budd, N.B. McKeown, D. Fritsch, Free volume and intrinsic microporosity in polymers, J. Mater. Chem. 15 (2005) 1977–1986.
[16] P. Budd, N. McKeown, B. Ghanem, K. Msayib, D. Fritsch, L. Starannikova, N. Belov, O. Sanfirova, Y. Yampolskii, V. Shantarovich, Gas permeation parameters and other physicochemical properties of a polymer of intrinsic microporosity: polybenzodioxane PIM-1, J. Membr. Sci. 325 (2008) 851–860.
[17] N.B. McKeown, P.M. Budd, Exploitation of intrinsic microporosity in polymer-based materials, Macromolecules 43 (2010) 5163–5176.
[18] C.R. Mason, L. Maynard-Atem, N.M. Al-Harbi, P.M. Budd, P. Bernardo, F. Bazzarelli, G. Clarizia, J.C. Jansen, Polymer of intrinsic microporosity incorporating thioamide functionality: preparation and gas transport properties, Macromolecules 44 (2011) 6471–6479.
[19] N. Du, G.P. Robertson, J. Song, I. Pinnau, S. Thomas, M.D. Guiver, Polymers of intrinsic microporosity containing trifluoromethyl and phenylsulfone groups as materials for membrane gas separation, Macromolecules 41 (2008) 9656–9662.
[20] N. Du, G.P. Robertson, I. Pinnau, M.D. Guiver, Polymers of intrinsic microporosity with dinaphthyl and thianthrene segments, Macromolecules 43 (2010) 8580–8587.
[21] P. Budd, K. Msayib, C. Tattershall, B. Ghanem, K. Reynolds, N. McKeown, D. Fritsch, Gas separation membranes from polymers of intrinsic microporosity, J. Membr. Sci. 251 (2005) 263–269.
[22] D. Fritsch, G. Bengtson, M. Carta, N.B. McKeown, Synthesis and gas permeation properties of spirobischromane-based polymers of intrinsic microporosity, Macromol. Chem. Phys. 212 (2011) 1137–1146.
[23] B.S. Ghanem, N.B. McKeown, P.M. Budd, D. Fritsch, Polymers of intrinsic microporosity derived from Bis(phenazyl) monomers, Macromolecules 41 (2008) 1640–1646.
[24] M. Carta, P. Bernardo, G. Clarizia, J.C. Jansen, N.B. McKeown, Gas Permeability of Hexaphenylbenzene Based Polymers of Intrinsic Microporosity, Macromolecules 47 (2014) 8320–8327.
[25] B.S. Ghanem, R. Swaidan, E. Litwiller, I. Pinnau, Ultra-microporous triptycene-based polyimide membranes for high-performance gas separation, Adv. Mater. 26 (2014) 3688–3692.
[26] B.S. Ghanem, R. Swaidan, X. Ma, E. Litwiller, I. Pinnau, Energy-efficient hydrogen separation by AB-type ladder-polymer molecular sieves, Adv. Mater. 26 (2014) 6696–6700.
[27] R. Swaidan, M. Al-Saeedi, B. Ghanem, E. Litwiller, I. Pinnau, Rational design of intrinsically ultramicroporous polyimides containing bridgehead-substituted triptycene for highly selective and permeable gas separation membranes, Macromolecules 47 (2014) 5104–5114.
[28] R. Swaidan, B. Ghanem, I. Pinnau, Fine-Tuned intrinsically ultramicroporous polymers redefine the permeability/selectivity upper bounds of membrane-based air and hydrogen separations, ACS Macro Lett. 4 (2015) 947–951.
[29] Y. Rogan, R. Malpass-Evans, M. Carta, M. Lee, J.C. Jansen, P. Bernardo, G. Clarizia, E. Tocci, K. Friess, M. Lanč, N.B. McKeown, A highly permeable polyimide with enhanced selectivity for membrane gas separations, J. Mater. Chem. A 2 (2014) 4874.
[30] Y. Zhuang, J.G. Seong, Y.S. Do, H.J. Jo, Z. Cui, J. Lee, Y.M. Lee, M.D. Guiver, Intrinsically microporous soluble polyimides incorporating Tröger's base for membrane gas separation, Macromolecules 47 (2014) 3254–3262.
[31] Z. Wang, D. Wang, J. Jin, Microporous polyimides with rationally designed chain structure achieving high performance for gas separation, Macromolecules 47 (2014) 7477–7483.
[32] M. Carta, M. Croad, R. Malpass-Evans, J.C. Jansen, P. Bernardo, G. Clarizia, K. Friess, M. Lanc, N.B. McKeown, Triptycene induced enhancement of membrane gas selectivity for microporous Troger's base polymers, Adv. Mater. 26 (2014) 3526–3531.
[33] M. Carta, R. Malpass-Evans, M. Croad, Y. Rogan, J.C. Jansen, P. Bernardo, F. Bazzarelli, N.B. McKeown, An efficient polymer molecular sieve for membrane gas separations, Science 339 (2013) 303–307.
[34] I. Rose, M. Carta, R. Malpass-Evans, M.-C. Ferrari, P. Bernardo, G. Clarizia, J.C. Jansen, N.B. McKeown, Highly Permeable Benzotriptycene-Based, Polym. Intrinsic Micro., ACS Macro Lett. 4 (2015) 912–915.
[35] H.B. Park, C.H. Jung, Y.M. Lee, A.J. Hill, S.J. Pas, S.T. Mudie, E. Van Wagner, B.D. Freeman, D.J. Cookson, Polymers with cavities tuned for fast selective transport of small molecules and ions, Science 318 (2007) 254–258.
[36] M. Calle, Y.M. Lee, Thermally rearranged (TR) Poly(ether–benzoxazole) membranes for gas separation, Macromolecules 44 (2011) 1156–1165.
[37] S. Li, H.J. Jo, S.H. Han, C.H. Park, S. Kim, P.M. Budd, Y.M. Lee, Mechanically robust thermally rearranged (TR) polymer membranes with spirobisindane for gas separation, J. Membr. Sci. 434 (2013) 137–147.
[38] Y.S. Do, J.G. Seong, S. Kim, J.G. Lee, Y.M. Lee, Thermally rearranged (TR) poly(benzoxazole-co-amide) membranes for hydrogen separation derived from

3,3′-dihydroxy-4,4′-diamino-biphenyl (HAB), 4,4′-oxydianiline (ODA) and isophthaloyl chloride (IPCl), J. Membr. Sci. 446 (2013) 294–302.
[39] Y.F. Yeong, H. Wang, K. Pallathadka Pramoda, T.-S. Chung, Thermal induced structural rearrangement of cardo-copolybenzoxazole membranes for enhanced gas transport properties, J. Membr. Sci. 397–398 (2012) 51–65.
[40] H. Wang, T.-S. Chung, The evolution of physicochemical and gas transport properties of thermally rearranged polyhydroxyamide (PHA), J. Membr. Sci. 385–386 (2011) 86–95.
[41] Y. Jiang, F.T. Willmore, D. Sanders, Z.P. Smith, C.P. Ribeiro, C.M. Doherty, A. Thornton, A.J. Hill, B.D. Freeman, I.C. Sanchez, Cavity size, sorption and transport characteristics of thermally rearranged (TR) polymers, Polymer 52 (2011) 2244–2254.
[42] S.H. Han, N. Misdan, S. Kim, C.M. Doherty, A.J. Hill, Y.M. Lee, Thermally rRearranged (TR) polybenzoxazole: effects of diverse imidization routes on physical properties and gas transport behaviors, Macromolecules 43 (2010) 7657–7667.
[43] S. Kim, H.J. Jo, Y.M. Lee, Sorption and transport of small gas molecules in thermally rearranged (TR) polybenzoxazole membranes based on 2,2-bis(3-amino-4-hydroxyphenyl)-hexafluoropropane (bisAPAF) and 4,4′-hexafluoroisopropylidene diphthalic anhydride (6FDA), J. Membr. Sci. 441 (2013) 1–8.
[44] S. Kim, K.T. Woo, J.M. Lee, J.R. Quay, M. Keith Murphy, Y.M. Lee, Gas sorption, diffusion, and permeation in thermally rearranged poly(benzoxazole-co-imide) membranes, J. Membr. Sci. 453 (2014) 556–565.
[45] I. Kardash, A.N. Pravednikov, Aromatic polyimides containing hydroxy and methyl groups, Vysok. Soyed 9 (1967) 873–876.
[46] G. Tullos, L. Mathias, Unexpected thermal conversion of hydroxy-containing polyimides to polybenzoxazoles, Polymer 40 (1999) 3463–3468.
[47] C.A. Scholes, C.P. Ribeiro, S.E. Kentish, B.D. Freeman, Thermal rearranged poly(benzoxazole-co-imide) membranes for CO_2 separation, J. Membr. Sci. 450 (2014) 72–80.
[48] W. Liu, W. Xie, Acetate-functional thermally rearranged polyimides based on 2,2-Bis(3-amino-4-hydroxyphenyl)hexafluoropropane and various dianhydrides for gas separations, Ind. Eng. Chem. Res. 53 (2014) 871–879.
[49] B. Comesaña-Gándara, M. Calle, H.J. Jo, A. Hernández, J.G. de la Campa, J. de Abajo, A.E. Lozano, Y.M. Lee, Thermally rearranged polybenzoxazoles membranes with biphenyl moieties: monomer isomeric effect, J. Membr. Sci. 450 (2014) 369–379.
[50] R. Guo, D.F. Sanders, Z.P. Smith, B.D. Freeman, D.R. Paul, J.E. McGrath, Synthesis and characterization of thermally rearranged (TR) polymers: effect of glass transition temperature of aromatic poly(hydroxyimide) precursors on TR process and gas permeation properties, J. Mater. Chem. A 1 (2013) 6063–6072.
[51] J.S. Chiou, D.R. Paul, Gas transport in a thermotropic liquid-crystalline polyester, J. Polym. Sci. Part B: Polym. Phys. 25 (1987) 1699–1707.
[52] J.C.I. Lara-Estévez, C. Camacho-Zuñiga, F.A. Ruiz-Treviño, E. Bucio, P.E. Cassidy, C.J. Booth, Gas transport properties of some fluorine-containing polyethers, Ind. Eng. Chem. Res. 49 (2010) 11948–11953.
[53] C.M. Zimmerman, W.J. Koros, Polypyrrolones for membrane gas separations. I. Structural comparison of gas transport and sorption properties, J. Polym. Sci. Part B: Polym. Phys. 37 (1999) 1235–1249.
[54] K. Tanaka, M. Okano, H. Toshino, H. Kita, K.-I. Okamoto, Effect of methyl substituents on permeability and permselectivity of gases in polyimides prepared from methyl-substituted phenylenediamines, J. Polym. Sci. Part B: Polym. Phys. 30 (1992) 907–914.
[55] Y.J. Cho, H.B. Park, High performance polyimide with high internal free volume elements, Macromol. Rapid Commun. 32 (2011) 579–586.
[56] K. Terada, K. Mizoguchi, T. Hirose, Gas transport in poly(vinyl methylbenzoates), J. Polym. Sci. Part B: Polym. Phys. 30 (1992) 539–548.
[57] K. Tanaka, H. Kita, K.-i. Okamoto, Permeability and permselectivity of gases in fluorinated polyimides, Sen.'i Gakkaishi 46 (1990) 541–547.
[58] M.W. Hellums, W.J. Koros, G.R. Husk, D.R. Paul, Gas transport in halogen-containing aromatic polycarbonates, J. Appl. Polym. Sci. 43 (1991) 1977–1986.
[59] J.-J. Shieh, T.-S. Chung, Gas permeability, diffusivity, and solubility of poly(4-vinylpyridine) film, J. Polym. Sci. Part B: Polym. Phys. 37 (1999) 2851–2861.
[60] N.A. Plate, S.G. Durgarjan, V.S. Khotimskii, V.V. Teplyakov, Y.P. Yampol'skii, Novel poly(silicon olefins) for gas separations, J. Membr. Sci. 52 (1990) 289–304.
[61] D.H. Weinkauf, D.R. Paul, Gas transport properties of thermotropic liquid-crystalline copolyesters. I. The effects of orientation and annealing, J. Polym. Sci. Part B: Polym. Phys. 30 (1992) 817–835.
[62] D.H. Weinkauf, D.R. Paul, Gas transport properties of liquid crystalline poly (ethylene terephthalate-co-p-oxybenzoate), J. Polym. Sci. Part B: Polym. Phys. 29 (1991) 329–340.
[63] F. Grün, Diffusionsmessungen an Kautschuk, Experientia 3 (1947) 490–492.
[64] R.W. Baker, B.T. Low, Gas separation membrane materials: a perspective, Macromolecules 47 (2014) 6999–7013.
[65] D.W. Breck, Zeolite Molecular Sieves: Structure, Chemistry, and Use, Wiley, New York, 1974.
[66] R.B. Bird, W.E. Stewart, E.N. Lightfoot, Transport Phenomena, 2nd ed., John Wiley & Sons, New York, NY, 1961.
[67] R.C. Reid, J.M. Prausnitz, T.K. Sherwood, The Properties of Gases and Liquids, McGraw Hill Book Co, New York, NY, 1977.
[68] M.M. Dal-Cin, A. Kumar, L. Layton, Revisiting the experimental and theoretical upper bounds of light pure gas selectivity–permeability for polymeric membranes, J. Membr. Sci. 323 (2008) 299–308.
[69] L.M. Robeson, B.D. Freeman, D.R. Paul, B.W. Rowe, An empirical correlation of gas permeability and permselectivity in polymers and its theoretical basis, J. Membr. Sci. 341 (2009) 178–185.
[70] V. Teplyakov, P. Meares, Correlation aspects of the selective gas permeabilities of polymeric materials and membranes, Gas. Sep. Purif. 4 (1990) 66–74.
[71] A. Alentiev, Y. Yampolskii, Correlation of gas permeability and diffusivity with selectivity: orientations of the clouds of the data points and the effects of temperature, Ind. Eng. Chem. Res. 52 (2013) 8864–8874.